

## **Evaluation of Rotation Correction Techniques for Electromagnetic Position Tracking Systems**

Volodymyr Kindratenko and Angela Bennett

National Center for Supercomputing Applications (NCSA), University of Illinois  
at Urbana-Champaign (UIUC), 405 North Mathews Avenue, Urbana, IL 61801, USA  
kindr@ncsa.uiuc.edu, ajbennet@uiuc.edu

**Abstract.** Electromagnetic position tracking devices are an integral part of many modern virtual reality systems. However, they have an inherent accuracy problem due to the dependence on the local electromagnetic field that can be easily distorted by a presence of magnetically active elements near the tracker's transmitter or receiver. Several analytical techniques have been proposed to overcome this limitation, however none of them is particularly good with the correction of rotation. In this work, we investigate various rotation correction algorithms in an attempt to identify the one that is most accurate and reliable.

### **1 Introduction**

A number of technologies can be used to track user's location and orientation in virtual reality applications [1]. To date, electromagnetic position tracking systems [2] have been the most widely used technology for various applications ranging from the head mounted displays to the immersive projection designs such as ImmersaDesks and CAVEs. Their high popularity is due to a number of factors, namely good accuracy within a relatively large tracking volume, nonexistence of the line-of-sight problem, light weight of the wearable part, etc. They are relatively inexpensive, readily available, and simple to install and use. However, they have an inherent accuracy problem due to the dependence on the local electromagnetic field that can be easily distorted by a presence of electrically or magnetically active elements near the tracker's transmitter or receiver [3]. Also, as working volume increases, their accuracy decreases. Several analytical techniques have been proposed to overcome these problems, an overview can be found in [4]. However, they mostly focus on the position correction and are not particularly good for the orientation correction. The purpose of this work therefore is to examine the existing rotation correction techniques, describe a new rotation correction framework, compare interpolation and high order polynomial fit approaches to identify the technique that is most accurate and reliable, and to point out some of the issues that have yet to be addressed.

### **2 Electromagnetic Tracking Principles**

Flock of Birds (Ascension Technology Corporation) and 3Space Fastrak (Polhemus,

Inc.) are among the most frequently used long-range electromagnetic tracking systems. Both devices are based on the design that uses orthogonal electromagnetic fields to sense 3D position and orientation [2]. The systems consist from an electromagnetic field transmitter coupled with a sensor via electronics linked to a computer. The electromagnetic transmitter contains three orthogonal coils that are pulsed in a sequence, the receiver also has three orthogonal coils that measure the electromagnetic field produced by the transmitter; the strength of the received signals is compared to the strength of the sent pulses to determine the position and compared to each other to determine the orientation. The systems differ in the manner in which the fields are generated and detected. 3Space Fastrak is referred to as an AC system because its transmitter uses bursts of sinusoidal current and the receiver contains passive coils in which currents are induced. Flock of Birds (FoB) is referred to as a DC system because it uses rectangular pulses of direct current and its receiver consists of orthogonal fluxgate sensors that measure the field. FoB makes three additional passive measurements per cycle in order to compensate for the constant magnetic field of the Earth. The measurements produced by both systems are rather noisy, therefore an additional filtering is implemented.

Working range of both systems is claimed to be up to 10 feet from the transmitter, but their accuracy significantly decreases as the distance between the transmitter and receiver increases. Also, due to the dependence of the measurements on the local electromagnetic field, they are sensitive to the ambient electromagnetic environment. If there is a metal, or other conductive material, or equipment that produces an electromagnetic field near the tracker's transmitter or receiver, the transmitter signals are distorted and the resulting measurements contain both static and dynamic error. Static errors as high as several feet have been observed near the maximum range of the tracking system. The manufacturers of the tracking systems suggest that there should be no metal components near the transmitter and receiver. This suggestion, however, is often not possible to implement due to the constructional limitations of many virtual reality systems and this also does not always cure the problem [5].

### **3 Tracker Calibration Principles**

One way to increase the accuracy of electromagnetic tracking systems is to compensate the measurements for the errors through experimentally established dependencies between the actual receiver position/orientation and that reported by the tracking system at some limited number of points. Assuming that the transmitter's position is fixed and the surrounding metal does not move, the static error is a function of the position of the receiver [2] (more on this follows) and it can be corrected as long as the magnetic field does not "fold back" on itself. Raab et al. [2] suggested that corrections of the distorted position and orientation measurements can take the form of additive vectors or a sequence of rotations and can be stored either in a look-up table or as polynomials in the position parameters. Much of the work done after [2] implements a variation of one of these two methods. However, the techniques found in the literature mostly focus on the position correction which is more noticeable in the applications, intuitive to understand and analyze, and less difficult to implement. Up to our knowledge, there are only three attempts reported in the literature to correct the rotation error.

Livingston et al. [5] recently demonstrated that the orientation error might as well be a function of both receiver's location and orientation. If this is the case, the complexity of the calibration problem rises significantly since not only more measurements are needed, but also different mathematics needs to be applied in order to design an appropriate calibration mechanism. We were unable to repeat the experiment described in [5] due to the absence of an appropriate measuring tool. Instead, we built a receiver holder that allows rotating the receiver around any of its 3 axes independently while maintaining the same location. The device is not very precise for determining the exact orientation, it only insures the axes of rotation. Therefore, the basic test is to rotate the receiver around one of its axes while keeping the other 2 constant – if the orientation error does not depend on the orientation, they should remain constant. We also supported this test with a visual inspection using a virtual reality application in which a virtual arrow was attached to the receiver so the changes in its orientation could be visually observed. Tests were conducted using FoB tracking system. Changes in both roll and yaw had no or very minor effect on the direction of the arrow, much less when moving the receiver away from the transmitter. Changes in pitch near  $+90^\circ$  and  $-90^\circ$  resulted in the arrow to change its orientation by  $180^\circ$ . Therefore, we concluded that the errors due to the rotation of the receiver are minor compared to the errors due to the changes in its location and in most cases can be neglected. However, this subject requires further investigation.

#### **4 Existing Rotation Correction Techniques**

Livingston et al. [5] described a method to correct errors in the rotation using averaging over the error quaternions of lookup table points surrounding the point to be calibrated. The lookup table is built by measuring a very large irregularly distributed set of samples within 2 meters from the transmitter and re-sampling it into a rectilinear grid to form calibration cells. The measurements are done with the help of Faro Metrecom IND-1 (Faro Technologies, Inc.) that provides a precise location/rotation of the receiver. Orientation errors were computed at each irregularly distributed point as the quaternion difference between the composed transformation from the receiver to itself as measured by Faro arm from one side and FoB from the other side and identity. During re-sampling, the errors were averaged by summing the matrices that correspond to the error rotations and computing the singular-value decomposition of the summed matrix. Once the rectilinear correction table is built, the error quaternion at the point to be calibrated is obtained by an interpolation of the error quaternions from the corners of the cell the point belongs to. It is done as a sequence of spherical linear interpolations, each between two quaternions. An example is supplied where the average orientation error is  $3.5^\circ$  before the correction and  $2.1^\circ$  afterwards. The error was measured as the angle through which the measured or corrected local coordinate system must rotate to match the true coordinate system. The authors conclude that such a poor performance is due to the dependence of the rotation error on the receiver's orientation.

There are some problems with this approach. The calibration table is not composed from the measured data, rather it is interpolated from it. As a result, the lookup table contains errors that were not present in the original data. Also, it is not clear how exactly the error quaternions are interpolated, e.g., in what order spherical

linear interpolations are applied, are there any weights associated with each vertex, what does “quaternion difference” mean, etc.

Ellis et al. [6] proposed to measure errors in the orientation by the quaternions that would rotate the measured local verticals, approximately surface normals to each quadrilateral patch, into true vertical. The receiver is placed at 8 known locations that form a cube that defines a single calibration cell and tracker readings are recorded at each location. The entire tracked volume is covered by the calibration cells of the same size. The orientation errors within each calibration cell are corrected by inverse rotations based on the error measurements at adjacent calibration grid nodes. The publication does not contain enough details to understand how exactly this is done. No results were published on the correction quality of this technique.

Kindratenko [4] used another technique based on the application of the high-order polynomial fit of the error rotation expressed in the form of Euler angles. Distorted position and rotation measurements are collected at some points of known true location and zero orientation of the receiver at each point. Fitting functions are built in the form of the high-order polynomials that fit the errors in Euler angles. Their coefficients are computed by solving the least square fit problem. Once the coefficients are known, the errors in yaw, pitch, and roll at a given tracked location are computed via the polynomials and corrected Euler angles are obtained rotating the tracked rotation by the fitted error rotation. Results show that the technique is efficient in removing large rotation distortions far from the transmitter and is less efficient in removing small distortions near the transmitter; in fact, it may occasionally introduce small additional errors near the transmitter.

One of the disadvantages of this approach is in expressing rotation via Euler angles – decomposing it into yaw, pitch, and roll and correcting each of them individually may not necessarily be a good idea. Also, one should be careful specifying the rotation axes since wrong rotation order leads to incorrect results. In addition, yaw, pitch, and roll are not necessarily well corrected by the polynomials of the same order, therefore it is preferable to identify the most appropriate polynomial order for each component individually, which was not originally done in [4].

## 5 Proposed Rotation Correction Framework

We use the notion of quaternions [7] since they eliminate many problems associated with Euler angles and rotation matrices. As receiver moves inside the tracked volume, it continuously reports its location  $(x, y, z)$  and rotation quaternion  $q = q_t q_{er}$  that contains both the true rotation quaternion  $q_t$  (the actual orientation of the receiver) and an error quaternion  $q_{er}$  the value of which is presumably a function of the receiver’s position. If  $q_{er}$  is known, the true quaternion is  $q_t = q q_{er}^{-1}$ . Therefore, our goal is to develop a technique that approximates the value of  $q_{er}$  at any given point  $(x, y, z)$  within the tracked volume with a sufficient accuracy based on a limited number of points for which we can experimentally measure  $q_{er}$ . One can notice that the techniques described in [4-6] also fit into this framework. Although they use different ways to represent the rotation, they all attempt to find  $q_{er}$  and use it to

compute the true quaternion  $q_i$  from the inverse rotation of  $q$  by  $q_{er}$ .

The following procedure is developed to compute  $q_{er}$ . First, place the receiver at 8 locations with known coordinates  $(x'_i, y'_i, z'_i)$ ,  $i = 1, \dots, 8$ , that form a cube and with known rotations  $q'_i$  (Fig. 1a). The tracking system reports coordinates  $(x_i, y_i, z_i)$  that form a polyhedron and rotations  $q_i$  that differ from  $q'_i$  by  $q''_i$  (Fig. 1b).

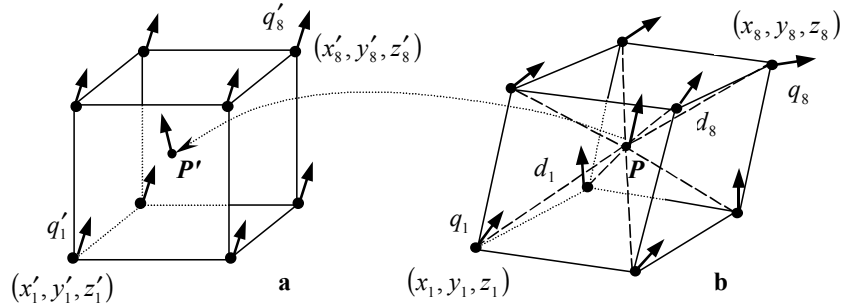


**Fig. 1.** Mapping between **a)** receiver placement points and **b)** tracker reported points.

Next, calculate error quaternions  $q''_i$  that rotate  $q'_i$  into  $q_i$  as  $q''_i = q_i^{-1} q'_i$ . Then the error quaternion  $q_{er}$  for any point  $(x, y, z)$  inside the tracked polyhedron can be interpolated based on the error quaternions  $q''_i$  at 8 corners of the cube as  $q_{er} = q'' / \|q''\|$  where  $q'' = \sum_{i=1}^8 q''_i w_i$  and  $w_i$  is the weight for the contribution of the error rotation at the vertex  $i$  to the overall error rotation at the location  $(x, y, z)$ . The weights  $w_i$  are scaled to insure that  $\sum_{i=1}^8 w_i = 1$ :  $w_i = f(d_i) / \sum_{j=1}^8 f(d_j)$  where  $d_i$  is the distance between the points  $(x, y, z)$  and  $(x_i, y_i, z_i)$  and  $f(d)$  can be defined as

$$f(d) = \begin{cases} 1 - \frac{d}{d_{\max}} & \text{if } d < d_{\max} \\ 0 & \text{if } d \geq d_{\max} \end{cases} \quad (1)$$

so the contribution of the error quaternion at a given vertex  $i$  decreases linearly as the distance between the points  $(x, y, z)$  and  $(x_i, y_i, z_i)$  increases. Alternative forms of  $f(d)$  to be evaluated are

$$f(d) = \begin{cases} 1 - \frac{d^2}{d_{\max}^2} & \text{if } d < d_{\max} \\ 0 & \text{if } d \geq d_{\max} \end{cases} \quad (2) \quad f(d) = \begin{cases} -\ln \frac{d}{d_{\max}} & \text{if } d < d_{\max} \\ 0 & \text{if } d \geq d_{\max} \end{cases} \quad (3)$$

where  $d_{\max}$  is a constant representing the distance starting from which the contribution of a given vertex vanishes. Its value is computed for each polyhedron as the half of the largest diagonal of the polyhedron. Note that if  $f(d) = \text{const} \neq 0$ , the result is the average of 8 error quaternions.

The entire tracked volume needs to be covered by the calibration cells in order to apply this technique. The size of the cells should be small enough to insure that the distortions of the magnetic field within each cell are linear or very close to linear. Also, a fast search algorithm is required to locate the polyhedron to which a point with the measured coordinates  $(x, y, z)$  belongs.

### 5.1 Calibration Table Measurements

The calibration table is built in the following way. We place the receiver at regularly spaced locations with known coordinates and with a known constant orientation and record both the known true position/rotation and that reported by the tracking system. We start from the front-bottom-left corner of the volume to be calibrated and first move along Z axis, then along X axis, and finally along Y axis with the same step size in all directions. The last point to be measured in this way is the back-upper-right corner of the tracked volume. The resulting calibration table contains tracker readings that are taken on the regular grid in the undistorted coordinates space.

It is very important to avoid any further magnetic field distortions while measuring the exact position of the sensor with the help of an alternative measuring technique. To achieve this, a simple sensor holder was designed consisting of a 1x1x0.1 foot wooden platform with a housing attached at the top and a set of plastic pipes of the length 2, 3, 4, 5, 6, and 7 feet that can be plugged into the housing (Fig. 2). Moving the platform on the regular grid marked on the floor and changing the pipes allows placing the sensor at the points whose locations can be precisely determined. After a very careful alignment, the precision of this measuring technique is  $\pm 5$  mm,  $\pm 1^\circ$ .

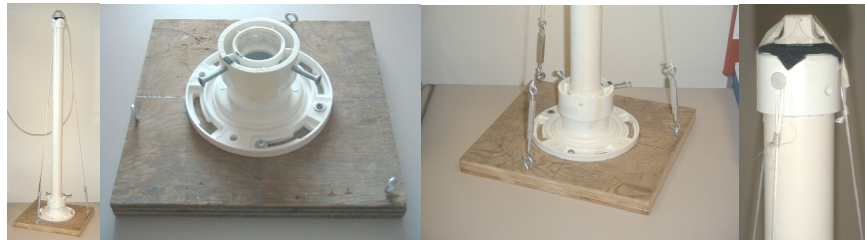


**Fig. 2.** Assembled sensor holder, wooden platform, and sensor attachment.

### 5.2 Polyhedron Search Algorithm

In order to compute the error quaternion at the point whose tracked coordinates are known, we need to identify its 8 surrounding points in the calibration table. The way

the calibration table is built provides us with a straightforward method of splitting the tracked volume into the polyhedrons whose corners are the needed 8 surrounding points. A test then is performed to verify if a given tracked point belongs to a given polyhedron. This is done by splitting each polyhedron into 5 tetrahedrons and verifying if the point belongs to one of them as described in [8]. If the point is outside the calibrated volume, it does not belong to any polyhedrons and therefore the nearest polyhedron is used. In practice, however, it is better to make sure that the calibration table is large enough to avoid this situation. Also, depending on the size of the calibration table, this search algorithm may become too slow to accommodate the needs of real-time tracking, therefore it is important to optimize it.

## 6 Comparison Study

Two techniques were used in the study: 3<sup>rd</sup> – 5<sup>th</sup> order polynomial fit as implemented in [4] and the above described interpolation using weighted error quaternions with the weights given by the equations 1-3. The algorithms were tested with two different tracking systems: Flock of Birds and Spacepad. The procedure is to use a calibration table to calculate polynomial coefficients for the fit, or as a lookup table for the interpolation, and to use a validation table to verify the accuracy of the rotation error correction. The calibration table for the FoB consists of the measurements taken at 432 locations below the FoB covering space 8x5x7 feet with 1-foot interval in each direction. The validation table consists of the measurements taken at 224 intermediate to the calibration table locations covering 7x3x6 feet volume. The calibration table for the Spacepad consists of the measurements taken at 140 locations directly below the Spacepad covering 6x3x4 feet volume. The validation table consists of the measurements taken at 48 intermediate to the calibration table locations covering 4x1x3 feet volume. The measurements were filtered by the utilities implemented in the electronics of each device. Therefore, it was enough to take only one measurement at each location since filtering removed the associated jitter very effectively making the errors due to the remaining jitter below the precision limits of our alternative measuring technique. Another issue to consider during the data acquisition is the size of the sampling distance. One-foot sampling interval may not be sufficient to accurately model the differences in the magnetic field changes from one location to another as linear and it may be necessary to increase the sampling density for the measurements taken further from the transmitter. This issue requires more study and is not addressed here.

Fig. 3 shows angular differences (computed as in [5]) for FoB between the actual orientation of the receiver and the orientation reported by the tracking system, between the actual orientation and the tracker readings corrected via the 4<sup>th</sup> order polynomial fit, and between the actual orientation and the tracker readings corrected via interpolation using the weights from eq. 2. Each group of consecutive 56 points corresponds to the measurements taken at the same distance from the floor. Connected dots show the changes in the angular difference as the receiver moves along Z axis. Improvements in the orientation precision are obvious from this plot. Similarly, Fig. 4 shows angular differences obtained for the Spacepad. Clearly, angular differences for corrected orientations are much smaller than for non-corrected.

Occasionally, however, both polynomial fit and interpolation produce values slightly larger than the non-corrected ones.

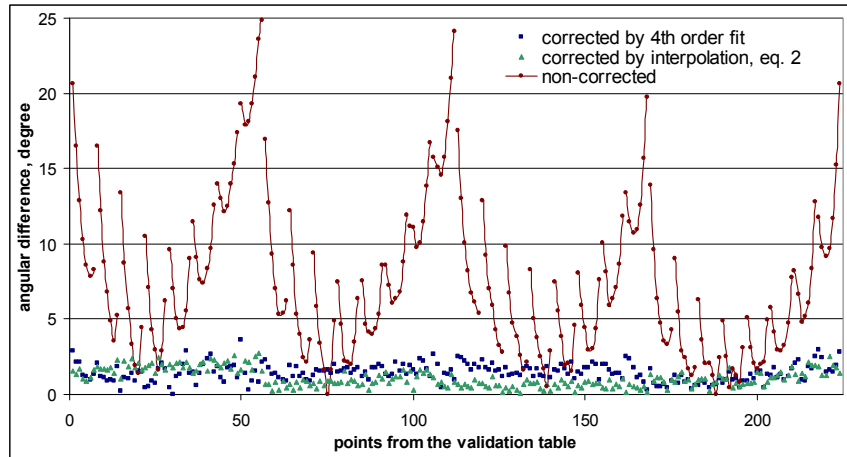


Fig. 3. Angular differences for non-corrected and corrected orientations, FoB.

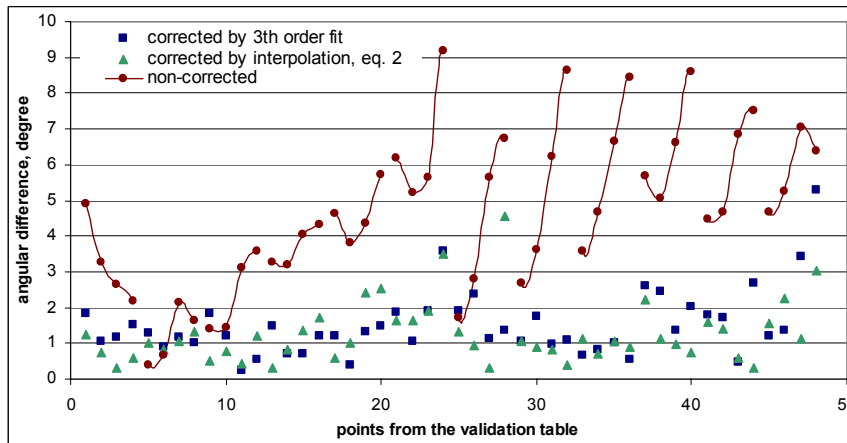


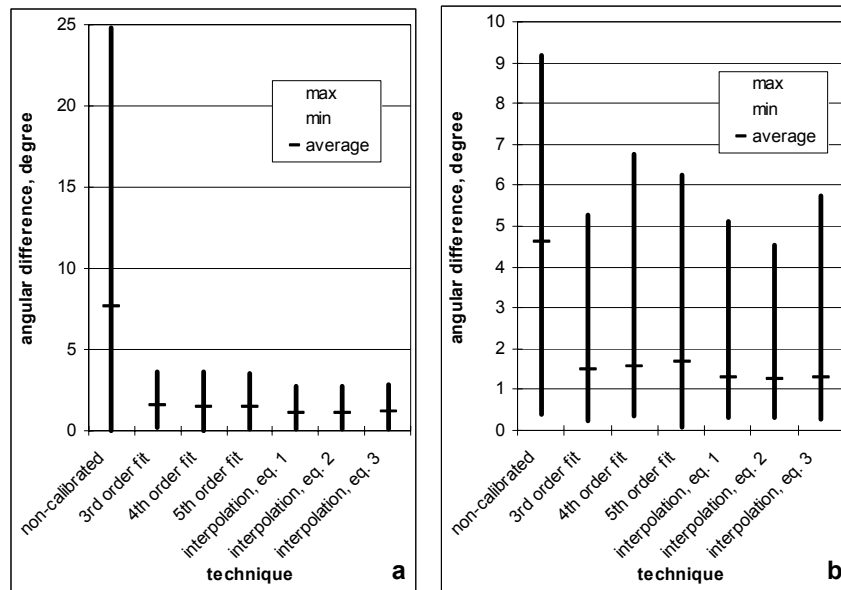
Fig. 4. Angular differences for non-corrected and corrected orientations, Spacepad.

Table 1 contains statistics obtained for both devices calibrated using all 6 calibration methods as well as for the non-calibrated validation tables. Fig. 5 shows min, average, and max values from the table for both datasets. In case of the FoB, the 5<sup>th</sup> order polynomial fit reduced the average angular difference from 7.6° for non-calibrated measurements to 1.5° for calibrated measurements. Interpolation-based

calibration using eq. 2 reduced this difference to 1.1°. As seen from Fig. 5a, both techniques performed well, interpolation produced just slightly better results.

**Table 1.** Statistics for non-calibrated and calibrated by all 6 techniques datasets.

Calibration method	FoB				Spacepad			
	avr, °	std, °	min, °	max, °	avr, °	std, °	min, °	max, °
non-calibrated	7.6	5.3	0.0	24.8	4.6	2.2	0.4	9.2
3 <sup>rd</sup> order fit	1.6	0.7	0.2	3.7	1.5	0.9	0.2	5.3
4 <sup>th</sup> order fit	1.4	0.6	0.0	3.6	1.6	1.0	0.4	6.8
5 <sup>th</sup> order fit	1.5	0.6	0.1	3.5	1.7	1.1	0.1	6.2
interpolation, eq. 1	1.1	0.6	0.1	2.8	1.3	0.9	0.3	5.1
interpolation, eq. 2	1.1	0.6	0.1	2.7	1.3	0.9	0.3	4.6
interpolation, eq. 3	1.1	0.6	0.1	2.8	1.3	1.0	0.3	5.8



**Fig. 5.** Min/average/max plots for a) Flock of Birds and b) Spacepad.

Both techniques performed good on the second dataset as well, with the interpolation achieving slightly better results (Fig. 5b). Average angular difference for the non-calibrated measurements is 4.6° and is only 1.3° after the interpolation using weights from eq. 2. The maximal values, however, have not decreased as much as for the FoB example. As seen from Fig. 4, angular differences for some points located near the edge of the calibration volume remain large even after the calibration. We observed that the distortions of the volume tracked with the FoB were more homogeneous than in the case of the Spacepad where different regions exhibited pronouncedly different shapes of the distortion with large changes inside some of the

calibration cells. This, probably, is the major reason for the poor interpolation of the measurements near the edge of the calibrated volume. Polynomial fit in this case also did not work well because the size of the calibration table is not big enough. In both cases, the solution is to obtain a more dense calibration table.

## 7 Concluding Remarks

Results show that both techniques can significantly reduce errors in the tracked rotation with the interpolation consistently producing slightly better results than the high-order polynomial fit. A more dense calibration table would help to eliminate the problems with the calibration near the edge of the tracked volume. Since both techniques require time-consuming measurements to obtain an adequate calibration table, the problem that remains unsolved is how to accelerate this to perform the calibration more rapidly. A software implementation of the techniques developed in this study is available at <http://www.ncsa.uiuc.edu/VPS/emtc/libtrcalib.htm>.

## Acknowledgements

This study is a collaboration between the National Center for Supercomputing Applications and the Integrated System Laboratory at the Beckman Institute, UIUC, with a financial support from Caterpillar, Inc. We are grateful to Prof. George Francis for his expertise in quaternionial algebra, Henry Kaczmarek for designing the devices used in the course of the study, and Rachael Brady for her support of this project.

## References

1. Meyer, K., Applewhite, H., Biocca, F.: A Survey of Position Trackers. *Presence* **1** (1992) 173-200
2. Raab, F., Blood, E., Steiner, T., Jones, H.: Magnetic Position and Orientation Tracking System. *IEEE Trans. Aerospace and Electronic Systems* **15** (1979) 709-718
3. Nixon, M., McCallum, B., Frigh, W., Price, B.: The Effects of Metals and Interfering Fields on Electromagnetic Trackers. *Presence* **7** (1998.) 204-218
4. Kindratenko, V.: Calibration of Electromagnetic Tracking Devices, *Virtual Reality* **4** (1999) 139-150
5. Livingston, M., State, A.: Magnetic Tracker Calibration for Improved Augmented Reality Registration. *Presence* **6** (1997) 532-546
6. Ellis, S., Adelstein, B., Baumeler, S., Jense, G., Jacoby, R.: Sensor Spatial Distortion, Visual Latency, and Update Rate Effects on 3D Tracking in Virtual Environments. In: *Proceedings IEEE Virtual Reality Conference* (1999) 218-221
7. Shoemake, K., Animating Rotation with Quaternion Curves, *Computer Graphics* **19** (1985), 245-254
8. Kenwright, D., Lane, D.: Interactive Time-Dependent Particle Tracing Using Tetrahedral Decomposition, *IEEE Trans. Visualization and Computer Graphics* **2** (1996) 120-129